

## Manipulating Deformable Linear Objects: Model-Based Adjustment-Motion for Vibration Reduction

Shigang YUE<sup>1</sup> and Dominik HENRICH

Embedded Systems and Robotics Lab. (RESY)  
Faculty of Informatics, University of Kaiserslautern  
D-67653 Kaiserslautern, Germany

[shigang, henrich]@informatik.uni-kl.de, Http: //resy.informatik.uni-kl.de/

### Abstract

This paper addresses the problem of handling deformable linear objects (DLOs) in a suitable way to avoid acute vibration. An adjustment-motion that eliminates vibration of DLOs and can be attached to the end of any arbitrary end-effector's trajectory is presented, based on the concept of open-loop control. The presented adjustment-motion is a kind of agile end-effector motion with limited scope. To describe the dynamics of deformable linear objects, the finite element method is used to derive the dynamic differential equations. Genetic algorithm is used to find the optimal adjustment-motion for each simulation example. In contrast to previous approaches, the presented method can be treated as one of the manipulation skills and can be applied to different cases without major changes to the method.

### 1. Introduction

Deformable materials such as cables, wires, ropes, cloths, rubber tubes, sheet metals, paper sheets and leather products can be found almost everywhere in the real world of industry and human activity. In most cases, deformable materials and parts are still handled and assembled by humans. Practical methods for the automatic handling and manipulation of deformable objects are urgently required.

Research involving the modeling and controlling of DLOs such as beams, cables, wires, and tubes etc. has been done. For example, Hirai *et al.* [1] presented a systematic approach to modeling of deformable soft parts for their manipulation, Nakagaki *et al.* [2] presented a method for calculating the force exerted on a wire based on stereo visual observations of its shape, while Zheng *et al.* [3] derived strategies to insert a flexible beam into a hole without sensors. However, the above methods are specialized and confined to limited applications.

Skill-based manipulation can generally be applied to various similar tasks. Skill-based manipulation for handling deformable linear materials has been touched upon recently. For example, Henrich *et al.* [4] analyzed the contact states and point contacts of DLOs with regard to manipulation skills, Abegg *et al.* [5] studied the contact state

transitions based on force and vision sensors and Remde *et al.* [6] discussed the problem of picking-up DLOs by experimentation.

However, the effects of dynamic vibration are not taken into account in the skill-related work described above. The dynamic effects of deformable objects cannot be neglected, especially when the objects are moved quickly by a robot arm. As shown in Figure 1, the uncertainty due to oscillation may cause failure in the insert-into-hole operation. Therefore, the vibration caused by inertia should be depressed during the motion or eliminated as soon as possible after the motion.

Vibration reduction of flexible structures has been a research topic for many researchers, and the previous works have been reviewed by Chen *et al.* [7]. Chen *et al.* also presented a passive approach based on open-loop concept for vibration-free handling of deformable beams; However, application of the method is limited, due to its stable start condition and relatively simple trajectory. Considering the complex manipulations involved in practice, such as avoiding obstacles, picking-up and insert-into-hole etc., a stable start condition cannot be satisfied easily.

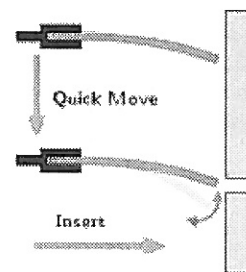


Figure 1: The vibration caused by quick operation results in uncertainty and failure, e.g., when inserting a DLO into a hole.

Therefore, a skill-based manipulation method to eliminate vibration of DLOs is presented in this paper. An adjustment-motion which can be attached to the end of an arbitrary trajectory of the end-effector is introduced. Adjustment-motion here refers to a kind of agile motion with limited scope. The attachable adjustment-motion can

<sup>1</sup> Shigang YUE is a research fellow of the Alexander von Humboldt Foundation from Beijing Polytechnic University

limited scope. The attachable adjustment-motion can be treated as one of the vibration-free manipulation skills. Vibration caused during the arbitrary previous trajectory can be reduced during the attached adjustment-motion. Our approach also uses an open-loop concept. The suitable adjustment motion can be found by applying optimization methods. Additionally, the adjustment-motion is chosen to be as simple as possible, so that it may be easily utilized.

The method here is model-based; no sensor is used.

## 2. Dynamic Modeling of DLOs

Finite element methods will be used in this paper to describe the dynamics of deformable linear objects [8,9]. Only the elastic deformation of DLOs is considered, plastic deformation will be disregarded.

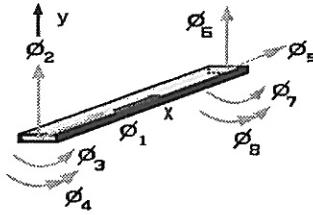


Figure 2: Parameters of a generalized element.

Figure 2 shows a generalized deformable element used here with eight parameters. The coordinates of the element are assembled in a vector form as:

$$\bar{\phi}_e = (\phi_1 \quad \phi_2 \quad \dots \quad \phi_8)^T \quad (1)$$

where  $\phi_1$  and  $\phi_5$  are the axial displacements along the  $x$ -axis,  $\phi_2$  and  $\phi_6$  are the transverse displacements along the  $y$ -axis,  $\phi_3$  and  $\phi_7$  are the rotary displacements about the  $z$ -axis, and  $\phi_4$  and  $\phi_8$  are the curvature displacements.

The longitudinal deformation  $D_{xe}$  and the transverse deformation  $D_{ye}$  at an arbitrary point  $p$  on the axis of an element can be expressed as follows:

$$D_{xe} = \bar{\phi}_e^T \bar{D}_x \quad (2)$$

$$D_{ye} = \bar{\phi}_e^T \bar{D}_y \quad (3)$$

where  $\bar{D}_x$  and  $\bar{D}_y$  are the vectors of the interpolation polynomials.

The velocity at point  $p$  is given by:

$$\bar{V}_p = [\bar{i} \quad \bar{j}] \begin{bmatrix} V_{ax} - \dot{q}D_{ye} + \dot{D}_{xe} \\ V_{ay} + \dot{q}(x + D_{xe}) + \dot{D}_{ye} \end{bmatrix} \quad (4)$$

where  $\bar{i}$  and  $\bar{j}$  are the unit vectors of the floating coordinate system that has  $x$  and  $y$  as axis and point  $a$  as origin,  $V_{ax}$  and  $V_{ay}$  are the projections of velocity at point  $a$  on the  $x$  and  $y$  axis respectively, and  $q$  is the joint angle.

The kinetic energy of a DLO element is expressible as:

$$T = \frac{1}{2} \int_0^L \lambda \bar{V}_p^2 dx \quad (5)$$

where  $\lambda$  is the mass of unit length, and  $L$  is the length of the element. Substitution of equations (2) and (3) into equation (4), and then substitution of equation (4) into equation (5), with subsequent rearrangement yields:

$$\begin{aligned} T = & \frac{1}{2} \lambda (V_{ax}^2 L + V_{ay}^2 L + \frac{1}{3} \dot{q}^2 L^3 + V_{ay} \dot{q} L^2) + \frac{1}{2} \lambda \dot{q}^2 \frac{LL}{A} \\ & + \frac{1}{2} \dot{q}^2 \bar{\phi}_e^T [m] \bar{\phi}_e + \frac{1}{2} \dot{\phi}_e^T [m^+] \dot{\phi}_e + \dot{q} \dot{\phi}_e^T [B] \bar{\phi}_e \\ & + \bar{\phi}_e^T \{y^+\} + \dot{\phi}_e^T \{x^+\} + \dot{q} \dot{\phi}_e^T \{z^+\} \end{aligned} \quad (6)$$

where

$$[m^+] = [m] + [m_z] \quad (7)$$

$$[m] = \lambda \int_0^L (\bar{D}_y \bar{D}_y^T + \bar{D}_x \bar{D}_x^T) dx \quad (8)$$

$$[B] = 2 \lambda \int_0^L (\bar{D}_y \bar{D}_x^T) dx \quad (9)$$

$$[m_z] = \frac{\lambda}{A} \int_0^L \left( \frac{\partial \bar{D}_y}{\partial x} \right) \left( \frac{\partial \bar{D}_y^T}{\partial x} \right) dx \quad (10)$$

$$\{y^+\} = \lambda \int_0^L (\dot{q}^2 x \bar{D}_x + V_{ay} \dot{q} \bar{D}_x - V_{ax} \dot{q} \bar{D}_y) dx \quad (11)$$

$$\{x^+\} = \lambda \int_0^L (\dot{q} y \bar{D}_y + V_{ay} \bar{D}_y + V_{ax} \bar{D}_x) dx \quad (12)$$

$$\{z^+\} = \frac{\lambda}{A} \int_0^L \left( \frac{\partial \bar{D}_y}{\partial x} \right) dx \quad (13)$$

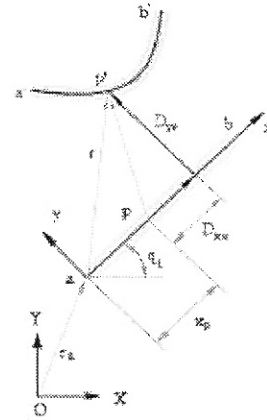


Figure 3: The deformation of a DLO element.

The potential energy of an element is the sum of the strain energy and the energy due to gravity, given by:

$$\begin{aligned} E_p = & \frac{1}{2} \int_0^L \{ EI \left( \frac{\partial^2 D_{ye}}{\partial x^2} \right)^2 + \frac{(EI)^2}{GA} \left( \frac{\partial^3 D_{ye}}{\partial x^3} \right)^2 + EA \left( \frac{\partial D_{xe}}{\partial x} \right)^2 \} dx \\ & + \lambda g \{ r_{ay} + \frac{1}{2} L \sin q_i + \int_0^L (D_{ye} \cos q_i + D_{xe} \sin q_i) dx \} \end{aligned} \quad (14)$$

where  $r_{ay}$  is the geometric projection of  $r_a$  (see Figure 3),  $r_a$  is a vector extending from the global frame to the beam fixed frame,  $E$  and  $G$  represent elastic and shear modulus respectively,  $A$  is the area of the link cross-section,  $I$  is the

second moment of area,  $A^*$  is the shear cross-sectional area, and  $g$  is the gravitational acceleration vector. With substitution of equations (2) and (3) into equation (14), the result can be expressed as:

$$E_p = \frac{1}{2} \bar{\phi}_e^T [K] \bar{\phi}_e + \lambda g (r_{av} + \frac{1}{2} L \sin q_i) + \lambda g \int_0^L \bar{\phi}_e^T (\bar{D}_y \cos q_i + \bar{D}_x \sin q_i) dx \quad (15)$$

The Lagrange equation for a DLO element is given as:

$$\frac{d}{dt} \left( \frac{\partial E_k}{\partial \dot{\bar{\phi}}_e} \right) - \frac{\partial E_k}{\partial \bar{\phi}_e} + \frac{\partial E_p}{\partial \bar{\phi}_e} = \bar{q}_e + \bar{f} \quad (16)$$

Substituting equations (6) and (15) into equation (16) and rearranging into a compact form gives:

$$[m_e] \ddot{\bar{\phi}}_e + [c_e] \dot{\bar{\phi}}_e + [k_e] \bar{\phi}_e = \bar{p}_e + \bar{f}_e \quad (17)$$

where

$$[m_e] = [m] + [m_z] \quad (18)$$

$$[c_e] = 2\dot{q}[B] \quad (19)$$

$$[k_e] = \dot{q}[B] - \dot{q}^2[m] + [k] \quad (20)$$

$$\bar{p}_e = \bar{y}^+ - \bar{x}^+ - \bar{z}^+ - \bar{m}_g \quad (21)$$

$$\bar{m}_g = \lambda g \int_0^L (\bar{D}_y \cos q_i + \bar{D}_x \sin q_i) dx \quad (22)$$

and  $\bar{f}_e$  is the external force given by the adjacent element.

The elemental dynamic equations can be assembled into a dynamic system and expressed in terms of global variables:

$$[M]_s \{\ddot{\Phi}\} + [C]_s \{\dot{\Phi}\} + [K]_s \{\Phi\} = \{P\}_s \quad (23)$$

where  $[M]_s$ ,  $[C]_s$ , and  $[K]_s$  are respectively the mass, damping, and stiffness matrix of the system and  $\{P\}_s$  is the load vector of the system.

### 3. Adjustment-Motion of End-effector

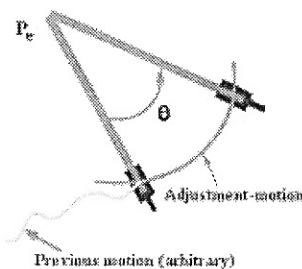


Figure 4: Adjustment motion of end-effector.

In a normal motion, DLOs go through an acceleration, constant velocity, and deceleration mode. Both acceleration and deceleration will cause vibration of DLOs. Most

previous research involved attempts to damp the vibration during the complete trajectory, for example in [7].

With regard to manipulation, only the vibration which could result in failure of the next operation must be eliminated. Most importantly, the vibration elimination method should be applicable in similar cases without necessitating major changes to the method. Based on the above requirements, we present an attachable adjustment-motion that can be conducted at the end of any arbitrary trajectory to damp the vibration caused by this previous motion.

As shown in Figure 4, the adjustment motion moves along a circle that assumes the nominal endpoint  $P_e$  of the DLO as its center and the length of the DLO as its radius. The adjustment-motion starts from the last nominal position of the previous arbitrary trajectory and ends at a certain point on the circle.

The profile of the adjustment-motion can be written as:

$$x = L \cos \theta + x_{ed} \quad (24)$$

$$y = L \sin \theta + y_{ed} \quad (25)$$

where  $x_{ed}$  and  $y_{ed}$  describe the nominal position of the endpoint  $p_e(x_{ed}, y_{ed})$  of the DLO. This point also acts as the center of the adjustment-motion.

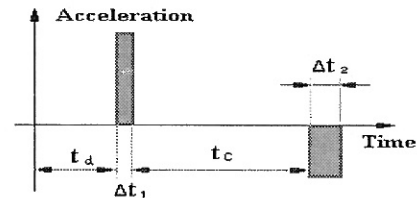


Figure 5: Acceleration profile of an adjustment-motion.

By using this adjustment motion, the DLO will be accelerated from rest to a velocity  $\omega$ . Then it is moved at this constant velocity for a certain period  $t_c$ . Deceleration is performed after this period to stop the adjustment motion.

There is a delay time  $t_d$  between the previous arbitrary end-effector's trajectory and adjustment-motion. The delay is useful in enabling the adjustment to take advantage of inertia.

For industrial robots, the period of acceleration and deceleration  $\Delta t$  is quite short. It is reasonable to assume that the movement of the DLOs involves a sharp increase in acceleration and deceleration. The profile of adjustment acceleration can be found in Figure 5, and

$$\omega = \varepsilon_{acc} \Delta t_1 \quad (26)$$

and

$$\omega = \varepsilon_{de} \Delta t_2 \quad (27)$$

where  $\varepsilon_{acc}$  and  $\varepsilon_{de}$  are the angular acceleration and deceleration, respectively.

The parameters of adjustment-motion that should be determined by optimization are as follows: delay time  $t_d$ , value of acceleration (negative is also possible)  $\varepsilon_{acc}$ , constant angular velocity  $\omega$ , running time at this velocity  $t_c$ , and the value of deceleration  $\varepsilon_{de}$ .

It follows that the scope of an adjustment-motion is determined by acceleration  $\epsilon_{acc}$ , deceleration  $\epsilon_{de}$ , angular velocity  $\omega$  and the running time  $t_c$ . Considering that the time of acceleration and deceleration  $\Delta t$  is quite small, the scope of an agile adjustment-motion is determined mainly by the running time  $t_c$ .

### 4. Adjustment-Motion Generation by Genetic Algorithms

The adjustment-motion generation problem for the vibration-free handling of DLOs can now be expressed as the following optimization problem:

$$\min : f = d_a \tag{28a}$$

$$s.t. \quad t_{d,min} \leq t_d \leq t_{d,max} \tag{28b}$$

$$\epsilon_{ac,min} \leq \epsilon_{ac} \leq \epsilon_{ac,max} \tag{28c}$$

$$\omega_{min} \leq \omega \leq \omega_{max} \tag{28d}$$

$$t_{c,min} \leq t_c \leq t_{c,max} \tag{28e}$$

$$\epsilon_{de,min} \leq \epsilon_{de} \leq \epsilon_{de,max} \tag{28f}$$

where  $d_a$  is the maximum amplitude of vibration,  $t_{d,min}$  and  $t_{d,max}$  are the lower and upper permitted delay times,  $\epsilon_{ac,min}$  and  $\epsilon_{ac,max}$  are the lower and upper permitted DLO angular accelerations,  $\omega_{min}$  and  $\omega_{max}$  are the lower and upper permitted DLO constant angular velocities,  $t_{c,min}$  and  $t_{c,max}$  are the lower and upper permitted running times at the constant angular velocity along the adjustment circle, and  $\epsilon_{de,min}$  and  $\epsilon_{de,max}$  are the lower and upper DLO angular decelerations, respectively. The maximum possible scope of adjustment-motion is controlled mainly by  $t_{c,max}$ .

Genetic Algorithms (GAs), are evolutionary, stochastic and global search methods. Their performance is superior to those of classical techniques [10] and they have been used successfully in robot path planning, for example [11]. We use genetic algorithms to determine the adjustment-motion parameters. GA programs can be founded described in detail [10].

### 5. Case Studies

To verify the above method, several case studies were conducted. One of the DLO's ends, which is grasped by the end-effector, was treated as a cantilever without vibrational deflection. The other distal end was treated as a free-end.

The cross section of the DLO was rectangular. The physical parameters of the DLO were: length 1.0m, width 11mm, height 0.5mm, elastic modulus  $1.26 \times 10^{11} Pa$ , shear modulus  $0.70 \times 10^{11} Pa$ , and density  $8960 Kg/m^3$ . All three cases were situated in the vertical plane. The gravitational acceleration was  $9.80 m/s^2$ .

The influence of the number of elements on the vibration of the DLO is shown in Figure 6. A lower number of elements does not result in vital error, but saves computing

time. In the following case studies, the DLO is described by two elements and a total of eight general coordinates.

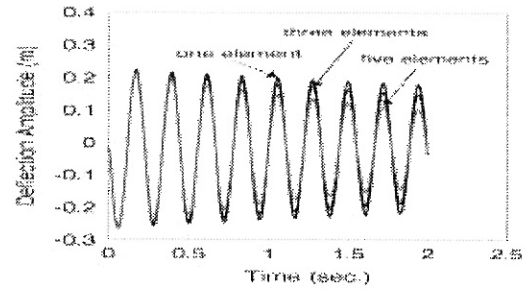


Figure 6: The influence of the number of elements on the endpoint vibration of a DLO, when the DLO is moved along an arc within one second and vibrates during the residual period.

#### 5.1 Case One

Suppose that the previous end-effector's motion was rotational. The adjustment-motion begins after the rotation (one second in duration) and a certain delay. In this case, the GA generated parameters were: delay time 0.047sec, value of acceleration  $-59.530 rad/s^2$ , constant angular velocity  $-2.401 rad/s$ , running time at this velocity 0.131sec and value of deceleration  $50.054 rad/s^2$ . The results are given in the following figures.

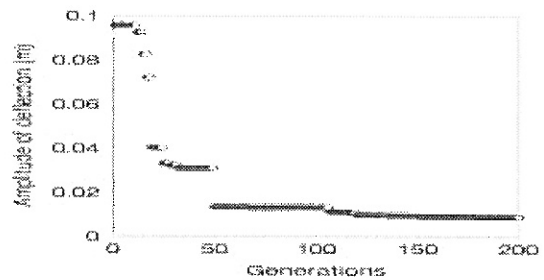


Figure 7: DLO's amplitude of deflection after adjustment-motion versus number of generations; the previous motion was rotation.

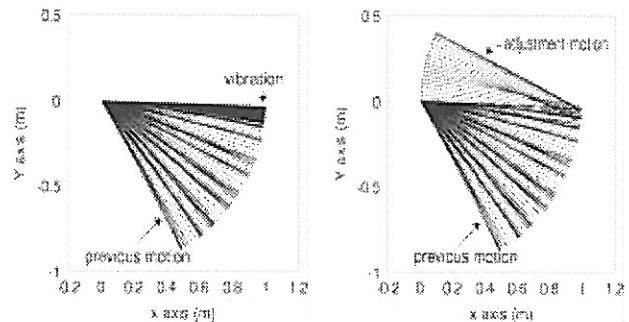


Figure 8: The previous motion, vibration and adjustment-motion of the DLO. Left: end-effector remains fixed after the previous rotation; right: end-effector adjusts after the previous rotation.

Figure 7 shows the vibrational amplitude versus the number of completed GA generations. The previous motion, vibration and adjustment-motion of the DLO are shown and compared in Figure 8. The vibration scope of the DLO during the residual period is clear for its overlapped black line as shown in the left part of Figure 8. The adjustment-motion was conducted immediately after the final position of the previous motion, as shown in the right part of Figure 8. A detailed comparison of the vibrational amplitudes resulting from these two situations is shown in Figure 9. It was found that the adjustment-motion can effectively reduce the vibrational amplitude. As shown in the figure, the vibrational amplitude was reduced sharply within 0.3sec.

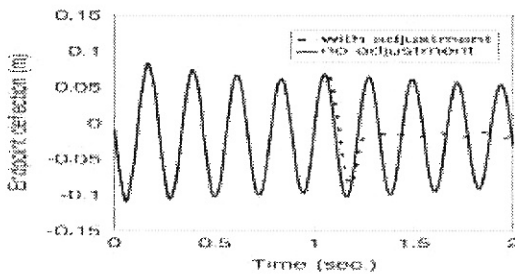


Figure 9: Endpoint deflection comparison of the DLO, the previous motion was rotation. Bold line: end-effector remains fixed after the previous motion; dashed line: end-effector adjusts after the previous motion.

5.2 Case Two

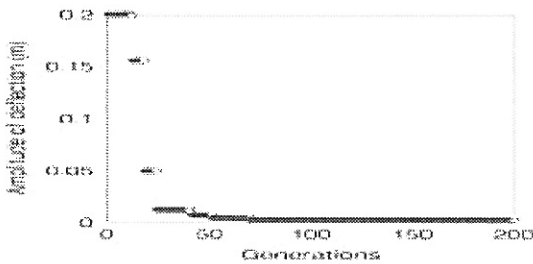


Figure 10: DLO's amplitude of deflection after adjustment-motion versus number of generations; the previous motion was translation.

Suppose the end-effector's previous motion was translation. The adjustment-motion begins after the previous translation (one second) and a certain delay. In this case, the GA generated parameters were: delay time 0.068sec, value of acceleration  $-96.481rad/s^2$ , constant angular velocity  $-3.001rad/s$ , running time at this velocity 0.117sec and value of deceleration  $56.789rad/s^2$ . The results are found in the following figures.

Figure 10 shows the vibrational amplitude versus number of completed GA generations. The previous motion, vibration and adjustment-motion of the DLO are shown and compared in Figure 11. A detailed comparison of the vibrational amplitude resulting from these two situations is

shown in Figure 12. It was again found that the adjustment-motion effectively reduces the vibrational amplitude.

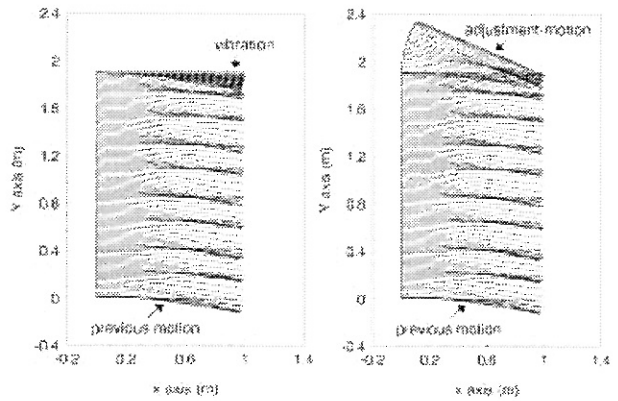


Figure 11: The previous motion, vibration and adjustment-motion of the DLO. Left: end-effector remains fixed after the previous translation; right: end-effector adjusts after the previous translation.

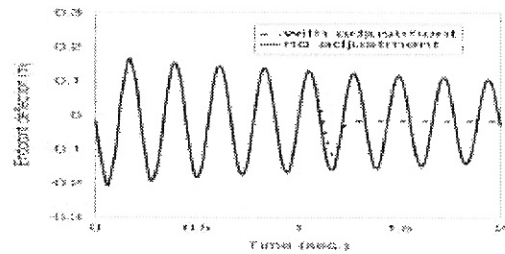


Figure 12: Endpoint deflection comparison of the DLO, the previous motion is translation. Bold line: end-effector remains fixed after the previous motion; dashed line: end-effector adjusts after the previous motion.

5.3 Case Three

To verify the effectiveness of this method based on a more general previous motion, we present here another case study. In this example, the previous motion (also of one second duration) combined rotation and translation. In case three, the GA generated parameters were: delay time 0.200sec, acceleration  $-97.263rad/s^2$ , constant angular velocity  $-4.000rad/s$ , running time at this velocity 0.164sec and deceleration  $57.971rad/s^2$ .

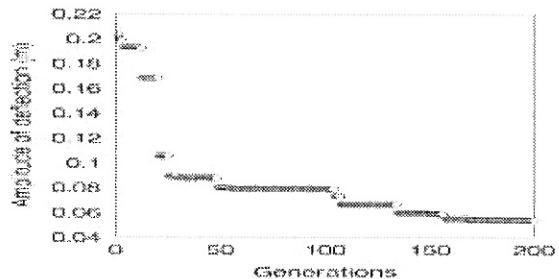


Figure 13: DLO's amplitude of deflection after adjustment-motion versus number of generations; the previous motion was combined rotation and translation.

The results are shown in Figures 13 through 15. It was once again found that the attached adjustment-motion is effective in reducing vibrations of the DLO. This implies that the adjustment-motion can be attached to any complex previous motions.

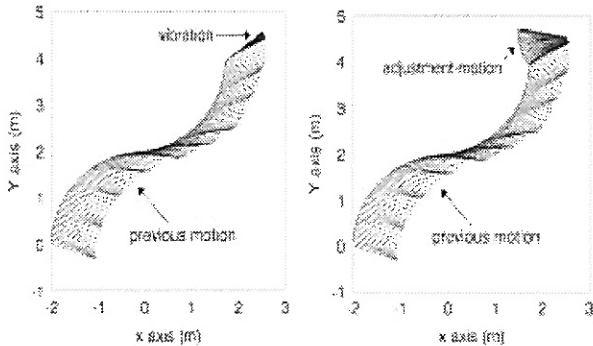


Figure 14: The previous motion, vibration and adjustment-motion of the DLO. Left, end-effector remains fixed after the previous motion; right, end-effector adjusts after the previous motion.

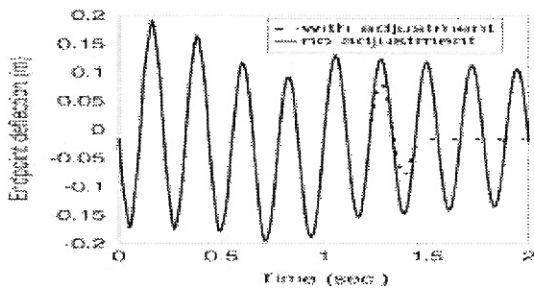


Figure 15: Endpoint deflection comparison of the DLO; the previous motion combined rotation and translation. Bold line: end-effector remains fixed after the previous motion; dashed line: end-effector adjusts after previous motion.

## 6. Conclusion

We have addressed the problem of manipulating deformable linear objects in a way suitable to avoid acute vibration. An adjustment-motion has been presented, which can be attached to the end of any arbitrary end effector's trajectory in order to eliminate unwanted vibration of the object. The case studies showed that an adjustment-motion is suitable for eliminating vibration arising during handling of deformable linear objects. Unlike previous approaches, the presented method can be treated as one of the manipulation skills, which are applicable to different practices without major changes to the method.

Although only one-dimensional objects were considered in this paper, the methods developed in the above sections may also be applied to two-dimensional objects.

In the future, an experiment based on the presented method will be performed and a two-way adjustment-motion that can maintain the original orientation and position of DLOs will be investigated.

## Acknowledgment

The support of the Alexander von Humboldt Foundation is greatly appreciated by the first author. We would like to thank Mr. Dirk EBERT for his kind help.

## References

- [1] Hirai S., Wakamatsu H. and Iwata K.: "Modeling of deformable thin parts for their manipulation". Proc. IEEE Int. Conf. On Robotics and Automation, vol.4, pp.2955-2960, San Diego, USA, May, 1994
- [2] Nakagaki H., Kitagaki K., Ogasawara T. and Tsukune H.: "Study of insertion task of a flexible beam into a hole by using visual tracking observed by stereo vision" Proc. Of IEEE Int. Conf. On Robotics and Automation, Vol.4, pp.3209-3214, Minneapolis, USA, April, 1996
- [3] Zheng Y.F., Pei R., and Chen C.: "Strategies for automatic assembly of deformable objects". Proc. IEEE Int. Conf. On Robotics and Automation, vol.3, pp.2598-2603, 1991
- [4] Henrich D., Ogasawara T. and Wörn H.: "Manipulating deformable linear objects -contact states and point contacts-". IEEE Int. Symposium on Assembly and Task Planning (ISATP'99), Porto,Portugal, July 21-24, 1999
- [5] Abegg F., Remde A. and Henrich D.: "Force and vision based detection of contact state transitions". 'Robot Manipulation of Deformable Objects', Edited by Henrich D. und Wörn H., Springer-Verlag, London, 2000
- [6] Remde A., Henrich D. and Wörn H.: "Picking-up deformable linear objects with industrial robots". Int. Symposium on Robotics (30<sup>th</sup> ISR), Tokyo, Japan, Oct.27-29, 1999
- [7] Chen Ming Z. and Zheng Yuan F.: "Vibration-Free handling of deformable beams by robot end-effectors". J. of Robotics Systems, pp.331-347, vol.12(5), 1995
- [8] Cleghorn W.L., Fenton R.G. and Tabarrok B.: "Finite element analysis of high-speed flexible mechanisms". Mechanism and Machine Theory, Vol.16(4), pp.407-424, 1981
- [9] Yue S.G. , Yu Y.Q. and Bai S.X.: "Flexible rotor beam element for manipulators with joint and link flexibility". Mechanism and Machine Theory, Vol.32(2),pp.209-219, 1997
- [10] Goldenberg D.E.: "Genetic Algorithms in search, optimization and machine learning". Addison-Wesley, Reading, Mass., 1989
- [11] Kubota N., Arakawa T., Fukuda T. and Shimojima K.: "Trajectory generation for redundant manipulator using virus evolutionary genetic algorithm". Proc. IEEE Int. Conf. On Robotics and Automation, vol.1, pp.205-210, New Mexico, USA, April, 1997